THERMAL SULFATE REDUCTION AS THE MAJOR CAUSE OF THE ANOMALOUSLY LOW RISE IN PALEOPROTEROZOIC OXYGEN

By

NATALIA LOUKINOVA

A thesis submitted in partial fulfillment of
the requirements of the degree of

MASTER OF SCIENCE IN GEOLOGY

WASHINGTON STATE UNIVERSITY
School of Earth and Environmental Sciences

MAY 2009

To the Faculty of Washington State University:

The members of the Committee appointed to examine the thesis of NATALIA LOUKINOVA find it satisfactory and recommend that it be accepted.

Dirk Schulze-Makuch, Ph.D., Co-Chair

Joan Wu, Ph.D., Co-Chair

Kent C. Keller, Ph.D.

ACKNOWLEDGEMENTS

I thank the members of my committee, namely, Dr. Dirk Schulze-Makuch, Dr. Joan Wu, and Dr. Kent C. Keller, for their guidance in my research. I specially thank Joan Wu for incessantly trying to raise me into a humble, responsible, and disciplined human being. I also thank my friend Pramod K. Pandey and my family for their concern and emotional support. This research was supported by the School of Earth and Environmental Sciences at Washington State University.

THERMAL SULFATE REDUCTION AS THE MAJOR CAUSE OF

THE ANOMALOUSLY LOW RISE IN PALEOPROTEROZOIC OXYGEN

Abstract

by Natalia Loukinova, M.S.
Washington State University
May 2009

Co-Chair: Dirk Schulze-Makuch

Co-Chair: Joan Wu

The first substantial rise in atmospheric pO_2 occurred during 2.3–2.0 Ga and could have been caused by the increase in burial of organic matter as suggested by the Lomagundi-Jatuli $\delta^{13}C$ positive excursion, which began sometime between 2.35 and 2.22 Ga and terminated at 2.058 Ga. The dilemma with the rise is that atmospheric pO_2 could not have risen higher than 0.2 PAL during that time despite the release of 10–16 PAL of excess oxygen into the atmosphere-ocean system. The oxygen consumption during the evolution of the exogenic sulfur cycle and on oxidation of ferrous iron during weathering of continental sedimentary rocks, presumed until now to have been responsible for the anomalously low rise, was not adequate. This study proposes that it was thermal sulfate reduction that restricted atmospheric pO_2 from rising above 0.2 PAL during 2.3–2.0 Ga. To compute the required rate of thermal sulfate reduction we developed an isotope mass balance model of the carbon and sulfur cycles and used the model to predict atmospheric pO_2 between 2.3 and 2.0 Ga. The rate was estimated to be roughly 4×10^{12} mol/yr with at least 65% of seawater sulfate being thermally reduced. The model results also

showed that the abundance of oceanic sulfate must have been higher during that time than at present, contrary to the notion of a sulfate-poor Paleoproterozoic ocean.

TABLE OF CONTENTS

Page

LIST OF TABLES

LIST OF FIGURES

INTRODUCTION

The Great Oxidation Event is a period roughly between 2.4 and 2.0 Ga marked by a substantial rise in atmospheric pO_2 (Holland 2006). Atmospheric pO_2 began to increase at 2.45 Ga when it exceeded 10^{-5} PAL as evidenced by the decrease in mass-independent fractionation in sulfur isotopes (Bekker et al. 2004). Photodissociation of volcanic SO_2 in an anoxic atmosphere caused mass-independent fractionation in sulfur isotopes and consequent formation of two reservoirs of miscellaneous photodissociation products with $\Delta^{33}S>0$ ‰ (water-insoluble sulfur species, e.g., elemental sulfur) and $\Delta^{33}S<0$ ‰ (water-soluble sulfur species, e.g., sulfite). The initial accumulation of oxygen in the atmosphere-ocean system at 2.45 Ga resulted in partial homogenation of the reservoirs, via oxidation of sulfur species from both, and a subsequent decrease in the magnitude of their $\Delta^{33}S$ (Farquhar et al. 2000). The atmosphere, however, remained poor in oxygen until 2.3–2.2 Ga as evidenced by the loss of iron from the upper zone of pre-2.25-Ga paleosols caused by the passage of oxygen-poor meteoric water that dissolved Fe^{2+}-bearing silicates and leached Fe^{2+} from the upper zone of soils (Holland 1999). In contrast, post-2.0-Ga paleosols were highly oxidized and retained all of their iron (Holland 1999). Hence, a dramatic rise in atmospheric pO_2 occurred between 2.3 and 2.0 Ga.

The oxygenation of the atmosphere between 2.3 and 2.0 Ga could have been caused by the increase in burial of organic matter as suggested by the Lomagundi-Jatuli $\delta^{13}C$ positive excursion (Petsch 2004). The Lomagundi-Jatuli event was the longest and largest perturbation in the carbon cycle in Earth's history (Melezhik et al. 2005). It began somewhere between 2.35 Ga (Shields and Veizer 2002) and 2.22 Ga (Karhu and Holland 1996) and terminated at 2.058±0.002 (±0.006) Ma (Melezhik et al. 2007) and attests to a 1.5-time increase in the rate of burial of

organic matter during that time. The dilemma with the rise in atmospheric pO_2 is that compared to the quantity of excess oxygen produced during that time, the level of atmospheric oxygen was anomalously low. Although, based on our model computations, 10–16 PAL of excess oxygen was released into the atmosphere-ocean system, atmospheric pO_2 could not have risen higher than 0.2 PAL, which is the larger of two upper estimates made by Kasting (1987) and Canfield and Teske (1996).

Kasting (1987) assumed the surface ocean to be a steady-state reservoir of oxygen with an input of oxygen through burial of organic matter and loss of oxygen through downwelling of surface water into the deep ocean and used Henry's Law, given by $P = \alpha C$, where P is atmospheric pO_2 and C is the concentration of oxygen in the surface ocean defined as the burial rate divided by the ocean mixing rate, to estimate the upper limit of atmospheric pO_2 to be 0.03 PAL. Canfield and Teske (1996) used Fick's law, given by $F = D\left(dC / dx\right)$, where F is the flux of oxygen to sediment surface, D is the diffusion coefficient of oxygen, and dC / dx is the gradient in concentration of dissolved oxygen (C) in the sediment-water boundary layer of thickness x, to estimate *carbon* required to oxygenate surface sediments (i.e., F meets or exceeds the rate of oxidation of organic matter in sediments) and hence establish the sulfide-oxygen interface required for the evolution of non-photosynthetic sulfide-oxidizing bacteria. The authors determined that bacterial evolution, which occurred in the Neoproterozoic era, became viable when atmospheric pO_2 exceeded 0.1–0.2 PAL (Canfield and Teske 1996).

To find a sink of oxygen that restricted atmospheric pO_2 from rising above 0.2 PAL during 2.3–2.0 Ga, it is necessary to consider other cycles correlated with the cycle of oxygen. Most important cycles are those of nitrogen, iron, and sulfur. In case of the nitrogen cycle, the appearance of oxygenic photosynthesis at 2.7 Ga initiated nitrification (oceanic ammonium is

oxidized by oxygen to nitrate) and denitrification (nitrate is reduced by an organic compound to gaseous N_2). Nitrification and subsequent denitrification reduced the net photosynthetic production of oxygen both by depleting fixed nitrogen (i.e., ammonium and nitrate) and hence forcing photosynthesizers to fix nitrogen themselves, which is more energy-intense than to assimilate fixed nitrogen directly, and by utilizing more oxygen to oxidize one mole of organic matter than released during photosynthesis of this one mole and, consequently, caused the delay in the rise of atmospheric pO_2, which became possible when nitrification exceeded denitrification (Fennel et al. 2005). This study deals with the oxygen rise rather than its delay and hence the oxygen consumption during the evolution of the nitrogen cycle is irrelevant.

The transformations in the sulfur and iron cycles are presumed to have kept atmospheric pO_2 from rising above 0.2 PAL during 2.3–2.0 Ga (Holland 2006). Prior to 2.3 Ga, the exogenic (sulfate-based) part of the sulfur cycle was not operational because, practically, all of the exogenic sulfur was in the form of volcanic SO_2 in the atmosphere and its photodissociation products in the ocean (Farquhar et al. 2000). The rise in atmospheric pO_2 resulted in oxidation of SO_2 and its photoproducts to sulfate and hence set off the exogenic sulfur cycle. The oxygen consumption on oxidation of exogenic sulfur destined for the *exogenic* recycling, however, must have been compensated by the oxygen production via microbial sulfate reduction and subsequent burial of sulfides, as determined in this study. As for the oxidation of Fe^{2+} during weathering of continental sedimentary rocks, although it could have contributed to the loss of at most 5–9 PAL of oxygen, i.e., the total mass of sedimentary rocks (the present value is 2.701×10^{24} g (Veizer 1988)) was eroded at a rate of 1.6 Ga^{-1} and contained, on average, 6% of iron that was oxidized at a stoichiometric ratio of 1 mol of Fe^{2+} to 1/4 mol of oxygen, it could not have been entirely

responsible for the anomalously low rise in atmospheric pO_2 during 2.3–2.0 Ga either. Therefore, there must have been some large sink of oxygen unknown until now.

This study proposes that it was the *endogenic* recycling of sulfur that kept atmospheric pO_2 from rising above 0.2 PAL during 2.3–2.0 Ga. To determine the required rate of thermal sulfate reduction, we developed an isotope mass balance model of the carbon and sulfur cycles and used the model to predict atmospheric pO_2 between 2.3 and 2.0 Ga.

METHODOLOGY

Oxygen and Cycles of Carbon and Sulfur

The carbon and sulfur cycles (Fig. 1 and 2) have a major influence on atmospheric pO_2 (Garrels and Lerman 1984). In the exogenic cycle, both elements move between sedimentary rocks by way of the atmosphere-ocean system. Carbon and sulfur exist in sedimentary rocks in reduced (organic carbon and sulfide) and oxidized (carbonate and sulfate) forms. As a result, the exogenic carbon cycle consists of the organic carbon and carbonate sub-cycles, and the exogenic sulfur cycle consists of the sulfide and sulfate sub-cycles. In the endogenic sulfur cycle, both elements cycle between the surface and interior of the Earth.

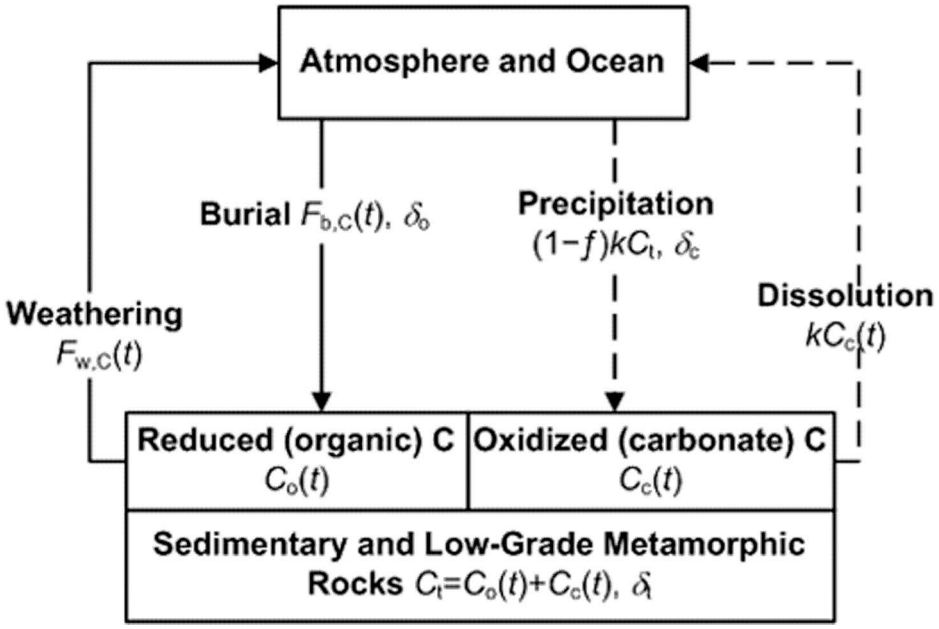

Fig. 1 Conceptual model of the organic (solid) and carbonate (dashed) carbon sub-cycles of the exogenic carbon cycle during 2.3–2.0 Ga

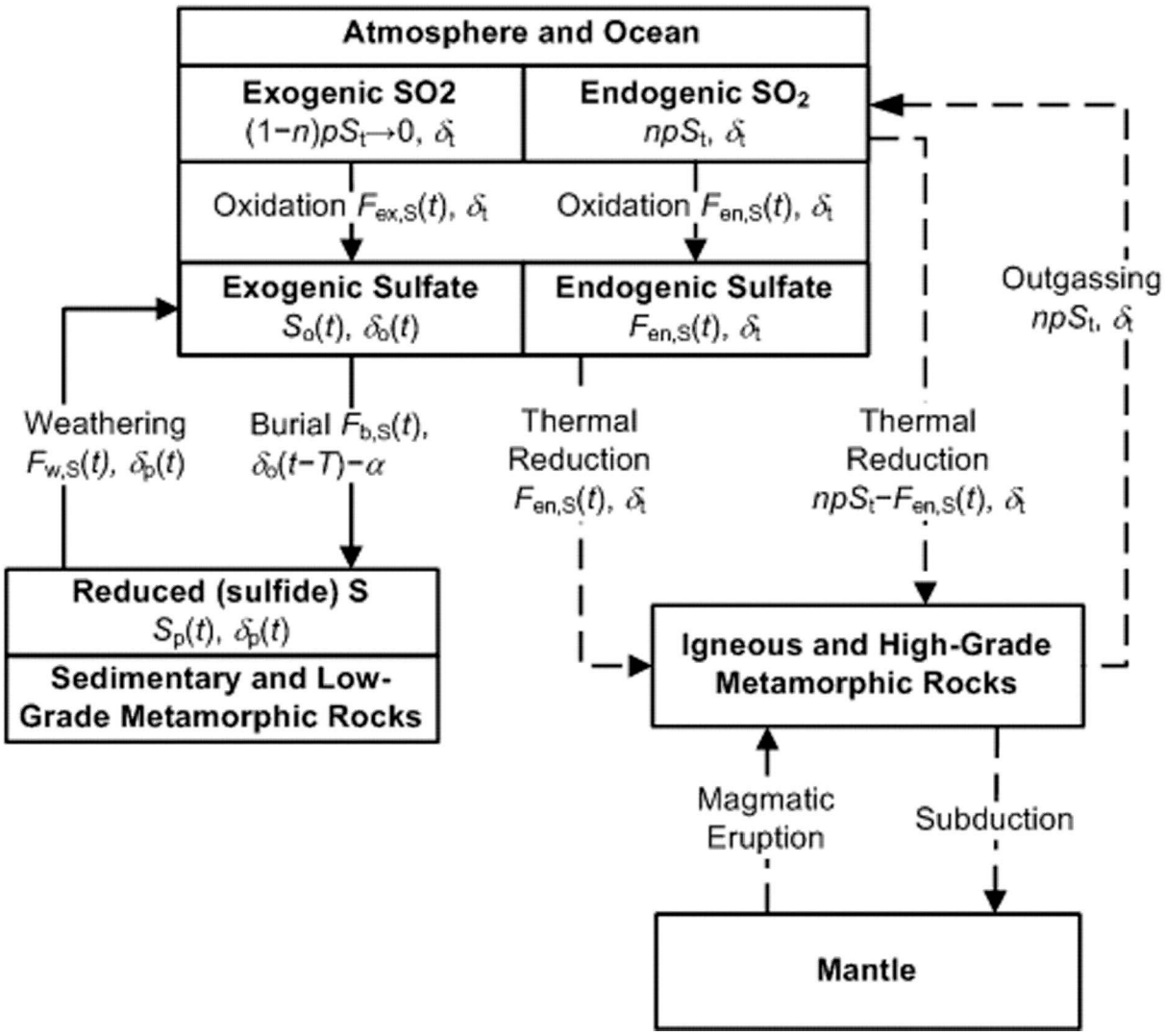

Fig. 2 Conceptual model of the exogenic (solid) and endogenic (dashed) sulfur cycles during 2.3–2.0 Ga

In the organic carbon sub-cycle, carbon is transferred from the atmosphere-ocean system into the organic carbon sub-reservoir via burial of organic matter, resulted from net photosynthesis (photosynthesis minus respiration), into sedimentary rocks. Oxygenic photosynthesis, the synthesis of organic matter from CO_2 and H_2O with the input of sunlight

energy accompanied by a release of oxygen as a by-product, can be represented by the simplified chemical reaction:

$$CO_2 + H_2O \rightarrow CH_2O + O_2, \quad (1)$$

where CH_2O denotes an organic compound in general. Respiration, microbial oxidation of organic matter, is the reverse of the reaction in Eqn. (1):

$$CH_2O + O_2 \rightarrow CO_2 + H_2O. \quad (2)$$

Carbon is transferred back into the atmosphere-ocean system via oxidative weathering of organic matter (Eqn. (2)), abiotic oxidation of old organic matter, exposed onto the surface by erosion of sedimentary rocks, by atmospheric oxygen.

In the sulfide sub-cycle, sulfur is transferred from the atmosphere-ocean system into the sulfide sub-reservoir via burial of sulfides, represented generally by pyrite (FeS_2), into sedimentary rocks. Formation of biogenic pyrite involves production of H_2S, via microbial sulfate reduction:

$$16CH_2O + 8SO_4^{2-} \rightarrow 8H_2S + 16HCO_3^-, \quad (3)$$

that subsequently reacts with detrital iron minerals such as Fe_2O_3:

$$2Fe_2O_3 + 8H_2S + O_2 \rightarrow 4FeS_2 + 8H_2O. \quad (4)$$

Sulfur is transferred back into the atmosphere-ocean system via oxidative weathering of sulfides:

$$15O_2 + 4FeS_2 + 8H_2O \rightarrow 2Fe_2O_3 + 8SO_4^{-2} + 16H^+ . \quad (5)$$

The burial of organic matter constitutes the production of oxygen because organic matter is hidden in sedimentary rocks from being oxidized. During microbial sulfate reduction, organic matter, derived via photosynthesis, is oxidized by sulfate, not by oxygen, leaving the original oxygen behind. Thus, the burial of sulfides also involves the release of oxygen. The oxidative weathering of organic matter and sulfides results in the uptake of oxygen and hence serves as a sink of oxygen.

In the endogenic sulfur cycle, during heating of seawater circulating in the axial hydrothermal cell at 350°C aqueous sulfate is reduced by basaltic ferrous iron to produce pyrite:

$$\underset{\text{Fayalite}}{11Fe_2SiO_4} + 2SO_4^{2-} + 4H^+ \rightarrow FeS_2 + \underset{\text{Magnetite}}{7Fe_3O_4} + 11SiO_2(aq) + 2H_2O \quad (6)$$

and

$$\underset{\text{Magnetite}}{15Fe_3O_4} + 2SO_4^{2-} + 4H^+ \rightarrow FeS_2 + \underset{\text{Hematite}}{22Fe_2O_3} + 2H_2O \quad (7)$$

(Shanks et al. 1981). Hydrothermal pyrite deposits, as part of the ocean floor, are subducted into the mantle where they are thermally decomposed to produce volcanic SO_2 that outgases into the atmosphere during a magmatic eruption:

$$4FeS_2 + 20H_2O + 4SiO_2 \rightarrow 8SO_2 + 20H_2 + 4FeSiO_3 \quad (8)$$

and is subsequently oxidized by atmospheric oxygen to sulfate:

$$8SO_2 + 4O_2 + 8H_2O \rightarrow 8SO_4^{2-} + 16H^+ \quad (9)$$

(Berner 2004), which is deposited back into the ocean. In contrast to microbial sulfate reduction (Eqn. (3)), where sulfate is reduced by an organic compound leaving behind the original (photosynthetic) oxygen that is subsequently consumed during oxidative weathering of biogenic pyrite, thermal sulfate reduction does not produce oxygen since sulfate is reduced by basaltic ferrous iron. Therefore, the oxidation of volcanic SO_2 produced as a result of a thermal breakdown of abiogenic, "seawater-derived" pyrite in the mantle is an absolute sink of oxygen.

Conceptual Model of Carbon Cycle

Practically, all of exogenic carbon resides in sedimentary rocks:

$$C_o(t) + C_c(t) = C_t, \quad (10)$$

where C_t is the present size of the sedimentary carbon reservoir taken from Garrels and Lerman (1984) to be 6.5×10^{21} mol, $C_c(t)$ and $C_o(t)$ are the carbonate and organic carbon sub-reservoirs, respectively, and t is geologic time (Ga). The atmosphere-ocean system serves solely as a reaction chamber where some fraction f of exogenic carbon entering the system is reduced to organic carbon. Assuming nonpreferential erosion, the mean $\delta^{13}C$ of exogenic carbon leaving the atmosphere-ocean system must be equal to that of sedimentary carbon, i.e., –5‰:

$$f\delta_o + (1-f)\delta_c = -5, \tag{11}$$

where δ_c and δ_o are $\delta^{13}C$ of carbonate and organic carbon, respectively, leaving the atmosphere-ocean system. The flux of carbon in and out of the atmosphere-ocean system (F_C) is defined as:

$$F_C(\text{mol/Ga}) = kC_t, \tag{12}$$

where k is an erosion rate of continental sedimentary mass taken from Veizer (1988) to be 16×10^{-10} yr^{-1}. Based on the previously made assumption of nonpreferential erosion, the rate of weathering of organic matter $(F_{w,C}(t))$ is obtained by substituting Eqn. (10) into (12):

$$F_{w,C}(t)(\text{mol/Ga}) = kC_o(t). \tag{13}$$

The rate of burial of organic matter $(F_{b,C})$ is defined as:

$$F_{\mathrm{b,C}}(\mathrm{mol/Ga}) = b_{\mathrm{C}} f = kC_{\mathrm{t}} f \ , \qquad (14)$$

where f was obtained by substituting δ_{c} and δ_{o} values taken from Karhu and Holland's (1996) into Eqn. (11) and solving Eqn. (11) for f. The mean values of f before and during the rise in atmospheric $p\mathrm{O}_2$ were estimated at 0.14 and 0.37, respectively.

Conceptual Model of Sulfur Cycle

The total mass of exogenic (sedimentary plus oceanic plus atmospheric) sulfur at t_0, where t_0 is the beginning time of the Lomagundi-Jatuli event ($2.22 \le t_0 \le 2.35$ Ga), was assumed to have been pS_{t}, where S_{t} is the present mass of exogenic S taken from Garrels and Lerman (1984) to be 4.42×10^{20} mol and p is some unknown fraction. A fraction n of pS_{t} was assumed to have been recycled exogenically; the remainder of exogenic sulfur was recycled endogenically. $(1-n)pS_{\mathrm{t}}$ moles of exogenic sulfur was recycled endogenically every T Ma, a time period required for the entire ocean to circulate through the axial hydrothermal cell.

The uncertainty ranges of T and p are $10 \le T \le 15.5$ Ma and $0 < p \le 0.16$, respectively. T is defined in (Stein et al. 1995) as $T = cT^{\circ}M_{\mathrm{o}} / Q_{\mathrm{h}}$, where c is the heat capacity of water, T° temperature of hydrothermal fluid in the axial cell, M_{o} total mass of the ocean, and Q_{h} hydrothermal heat flow. Q_{h} was 2–3 times greater at 2.3 Ga than at present (Lowell and Keller 2003). Hence, T must have been 1/2–1/3 times the present value of 31 Ma. Since whatever exogenic sulfur was oxidized during the initial accumulation of atmospheric oxygen had to be

deposited into the ocean, the upper bound of p was constrained by the maximum solubility of sulfate ($c_{\max}$ taken from Fig. 3.6 in Freeze and Cherry (1979) at 51 mmol/kg) to be $c_{\max} M_{\mathrm{o}} / S_{\mathrm{t}}$.

Endogenic Sulfur Cycle

The endogenically recycled sulfur did not necessarily have to be in the form of sulfate. Prior to the rise in atmospheric pO_2, it was in the form of products of photodissociation of volcanic SO_2. For the purpose of computing the oxygen consumption, however, the rate of thermal reduction of *sulfate* ($F_{\mathrm{en,S}}(t)$) is of interest:

$$F_{\mathrm{en,S}}(t)(\mathrm{mol}/T\ \mathrm{Ma}) = \min(npS_{\mathrm{t}}, M(t)/(1/2)), \tag{15}$$

where $M(t)$ is the quantity of oxygen in the atmosphere-ocean system (mol) and, in addition to the previous definition, T is the model time step. The mean $\delta^{34}\mathrm{S}$ of exogenic sulfur (δ_{t}) is close to the magmatic $\delta^{34}\mathrm{S}$, i.e., +2‰ (Hayes et al. 1992). To maintain δ_{t} at +2‰ it was assumed that sulfur isotopic fractionations imparted by various processes during the endogenic recycling of exogenic sulfur cancelled each other out.

Exogenic Sulfur Cycle

Due to the comparability in the size of the sedimentary and oceanic sulfur reservoirs and hence inapplicability of the isotope mass balance model of the carbon cycle to the exogenic sulfur cycle, the isotope mass balance model of Garrels and Lerman (1984) was adopted with a

few modifications. First, to capture the evolution of the exogenic-part of the sulfur cycle initiated by the rise in atmospheric pO_2 the oxidation of products of photodissociation of volcanic SO_2 to oceanic sulfate destined for the exogenic recycling $(F_{ex,S}(t))$ was introduced into their model. Second, due to the absence of massive sulfate evaporites of the Paleoproterozoic age (Strauss 2004), their deposition was assumed to have been minimal during that time, and the sulfate sub-cycle was removed from the Garrels and Lerman (1984) model. Thus, in the model the exogenic sulfur exists in the form of volcanic SO_2 and its photodissociation products (at the initial stage), oceanic sulfate, and sedimentary sulfides.

The main conditions of the model are:

$$S_p(t) + S_o(t) \le (1-n)\,pS_t\,, \tag{16}$$

$$\delta_p(t)S_p(t) + \delta_o(t)S_o(t) = \delta_t(S_p(t) + S_o(t))\,, \tag{17}$$

where $S_p(t)$ is the sedimentary sulfide reservoir (mol), $S_o(t)$ is the reservoir of oceanic sulfate recycled exogenically (mol), $\delta_p(t)$ and $\delta_o(t)$ are the mean $\delta^{34}S$ of $S_p(t)$ and $S_o(t)$, respectively.

The changes in the masses of $S_o(t)$ and $S_p(t)$ ($\frac{dS_o(t)}{dt}$ and $\frac{dS_p(t)}{dt}$, respectively) are:

$$\frac{dS_o(t)}{dt} = F_{w,S}(t) - F_{b,S}(t) + F_{ex,S}(t)\,, \tag{18}$$

$$\frac{dS_{\mathrm{p}}(t)}{dt} = -\left[\frac{dS_{\mathrm{o}}(t)}{dt} - F_{\mathrm{ex,S}}(t)\right] = F_{\mathrm{b,S}}(t) - F_{\mathrm{w,S}}(t), \tag{19}$$

where $F_{\mathrm{b,S}}(t)$ is the rate of burial of sulfides, $F_{\mathrm{w,S}}(t)$ is the rate of oxidative weathering of sulfides defined as:

$$F_{\mathrm{w,S}}(t)(\mathrm{mol}/T\ \mathrm{Ma}) = kS_{\mathrm{p}}(t), \tag{20}$$

and $F_{\mathrm{ex,S}}(t)$ is defined as:

$$F_{\mathrm{ex,S}}(t)(\mathrm{mol}/T\ \mathrm{Ma}) = \min((1-n)pS_{\mathrm{t}} - S_{\mathrm{o}}(t) - S_{\mathrm{p}}(t), M(t)/(1/2)). \tag{21}$$

$\delta^{34}\mathrm{S}$ of evaporitic sulfates, which record $\delta_{\mathrm{o}}(t)$, gradually increased from +2‰ in the Late Archean to +25‰ in the late Paleoproterozoic (Hayes et al. 1992; Strauss 1993). Because of the fragmentary nature of this sulfate-sulfur isotopic record, the internal structure of this increase is unknown (Strauss 2004). Thus, for simplicity, a linear temporal trend (+2‰ at t_0 to +25‰ at 1.6 Ga) is assumed:

$$\delta_{\mathrm{o}}(t) = \frac{25-2}{1.6-t_0}(t-t_0) + 2. \tag{22}$$

The isotopic fractionation between coeval sulfates and sulfides (α) imparted by microbial sulfate reduction was randomly chosen from the range of the possible Paleoproterozoic α values

(2–25‰) to be 20‰ (Hayes et al. 1992). The change in the isotope mass of $S_o(t)$ ($\frac{d\delta_o(t)S_o(t)}{dt}$) is defined as:

$$\frac{d\delta_o(t)S_o(t)}{dt} = \delta_p(t)F_{w,S}(t) - \left(\delta_o(t-T) - \alpha\right)F_{b,S}(t) + \delta_t F_{ex,S}(t). \quad (23)$$

$\frac{d\delta_o(t)S_o(t)}{dt}$ is also defined as:

$$\begin{aligned}
&\frac{d\delta_o(t)S_o(t)}{dt} = \frac{\delta_o(t-T)S_o(t-T) - \delta_o(t)S_o(t)}{T} = \\
&\frac{1}{T}\left[\left(\delta_o(t) + \frac{d\delta_o(t)}{dt}\right)\left(S_o(t) + \frac{dS_o(t)}{dt}\right) - \delta_o(t)S_o(t)\right] = \\
&\frac{1}{T}\left[\frac{d\delta_o(t)}{dt}S_o(t) + \frac{dS_o(t)}{dt}\left(\delta_o(t) + \frac{d\delta_o(t)}{dt}\right)\right] = \\
&\frac{1}{T}\left[\frac{d\delta_o(t)}{dt}S_o(t) + \frac{dS_o(t)}{dt}\delta_o(t-T)\right].
\end{aligned} \quad (24)$$

Substituting Eqn. (18) into (24), combining Eqn. (23) and (24), and solving for $F_{b,S}(t)$ yield:

$$F_{b,S}(t)(\text{mol}/T\ \text{Ma}) = \frac{1}{\alpha}\left[\frac{d\delta_o(t)}{dt}S_o(t) + (\delta_o(t-T) - \delta_p(t))F_{w,S}(t) + (\delta_o(t-T) - \delta_t)F_{ex,S}(t)\right]. \quad (25)$$

Differentiating Eqn. (17) one obtains:

$$\frac{d\delta_{\mathrm{p}}(t)S_{\mathrm{p}}(t)}{dt} = \delta_{\mathrm{t}}F_{\mathrm{ex,S}}(t) - \frac{d\delta_{\mathrm{o}}(t)S_{\mathrm{o}}(t)}{dt}. \tag{26}$$

$\frac{d\delta_{\mathrm{p}}(t)S_{\mathrm{p}}(t)}{dt}$ is also defined as:

$$\begin{aligned}
&\frac{d\delta_{\mathrm{p}}(t)S_{\mathrm{p}}(t)}{dt} = \frac{\delta_{\mathrm{p}}(t-T)S_{\mathrm{p}}(t-T) - \delta_{\mathrm{p}}(t)S_{\mathrm{p}}(t)}{T} = \\
&\frac{1}{T}\left[\left(\delta_{\mathrm{p}}(t) + \frac{d\delta_{\mathrm{p}}(t)}{dt}\right)\left(S_{\mathrm{p}}(t) + \frac{dS_{\mathrm{p}}(t)}{dt}\right) - \delta_{\mathrm{p}}(t)S_{\mathrm{p}}(t)\right] = \\
&\frac{1}{T}\left[\delta_{\mathrm{p}}(t)\frac{dS_{\mathrm{p}}(t)}{dt} + \frac{d\delta_{\mathrm{p}}(t)}{dt}\left(S_{\mathrm{p}}(t) + \frac{dS_{\mathrm{p}}(t)}{dt}\right)\right] = \\
&\frac{1}{T}\left[\delta_{\mathrm{p}}(t)\frac{dS_{\mathrm{p}}(t)}{dt} + \frac{d\delta_{\mathrm{p}}(t)}{dt}S_{\mathrm{p}}(t-T)\right].
\end{aligned} \tag{27}$$

Combining Eqn. (26) and (27) and solving for $\frac{d\delta_{\mathrm{p}}(t)}{dt}$ yield:

$$\begin{aligned}
&\frac{d\delta_{\mathrm{p}}(t)}{dt} = \frac{1}{S_{\mathrm{p}}(t-T)}\left[\delta_{\mathrm{t}}F_{\mathrm{ex,S}}(t) - \frac{d\delta_{\mathrm{o}}(t)S_{\mathrm{o}}(t)}{dt} - \delta_{\mathrm{p}}(t)\frac{dS_{\mathrm{p}}(t)}{dt}\right] = \\
&(\delta_{\mathrm{o}}(t-T) - \alpha)F_{\mathrm{b,S}}(t) - \delta_{\mathrm{p}}(t)F_{\mathrm{b,S}}(t).
\end{aligned} \tag{28}$$

Atmospheric pO_2

The change in the quantity of oxygen in the atmosphere-ocean system $(\frac{dM(t)}{dt})$ is a balance between the production and consumption fluxes, as given by the following equation:

$$\frac{dM(t)}{dt} = \left[F_{\mathrm{b,C}}(t) - F_{\mathrm{w,C}}(t) \right] + \frac{15}{8}\left[F_{\mathrm{b,S}}(t) - F_{\mathrm{w,S}}(t) \right] - \frac{1}{2}\left[F_{\mathrm{ex,S}}(t) + F_{\mathrm{en,S}}(t) \right], \quad (29)$$

where 15/8 and 1/2 are stoichiometric ratios of oxygen to sulfide (Eqn. (3) and (4) for $F_{\mathrm{b,S}}(t)$ and Eqn. (5) for $F_{\mathrm{w,S}}(t)$) and oxygen to SO_2 (Eqn. (9)), respectively. Appendix A explains how to compute the atmospheric pO_2 (PAL) based on the mass of oxygen (mol) in the atmosphere-ocean system.

Model Implementation

The mathematical model was implemented in C++ (Appendix B). The model spans the period from t_0, where **(** $2.22 \le t_0 \le 2.35$ Ga), to 2.058 Ga. For convenience, the time step is set to *T*. Hence, each time step the ocean circulates through the axial (high-temperature) hydrothermal cell once. The flowchart of the computer model is depicted in Fig. 3.

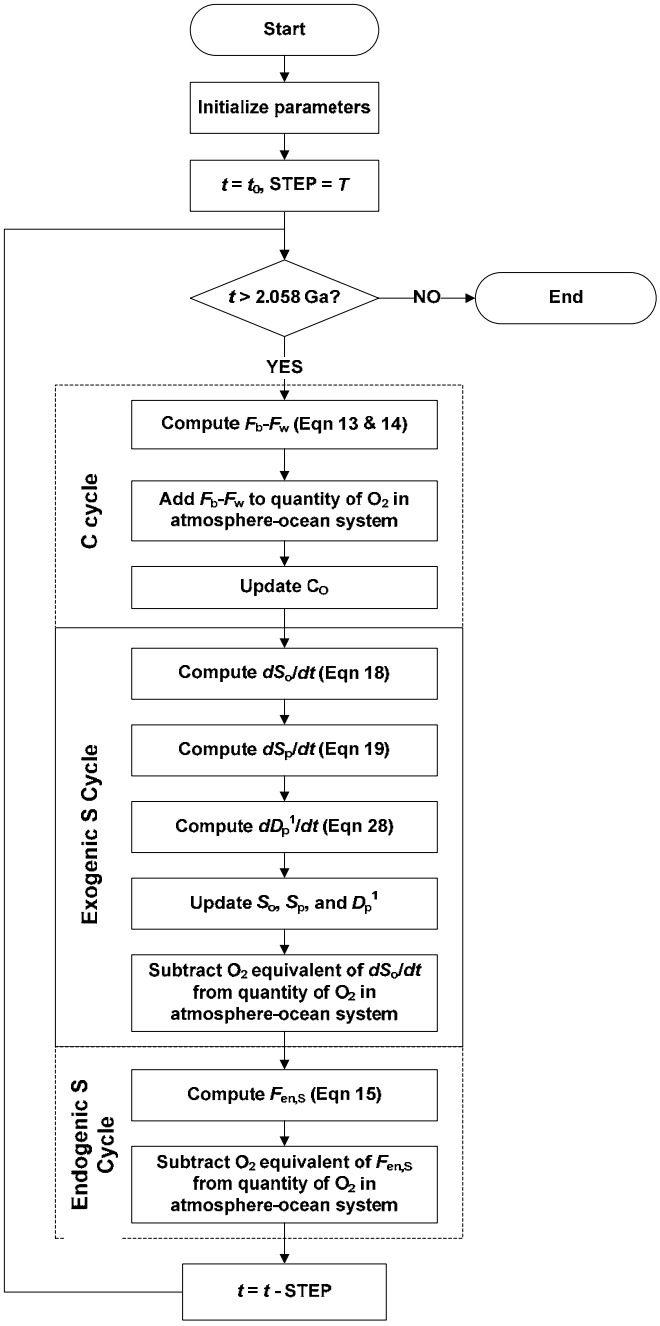

Fig. 3 Model flowchart. [1] D_p denotes δ_p

RESULTS AND DISCUSSION

Based on the Paleoproterozoic paleosol record, the first substantial rise in atmospheric pO_2 occurred during 2.3–2.0 (Holland 1999) and, as suggested by the Lomagundi-Jatuli $\delta^{13}C$ positive excursion, which started somewhere between 2.35 Ga (Shields and Veizer 2002) and 2.22 Ga (Karhu and Holland 1996) and ended at 2.058±0.002 (±0.006) Ma (Melezhik et al. 2007), was likely to have been caused by the increase in burial of organic matter (Petsch 2004). Despite the release of 10–16 PAL of excess oxygen into the atmosphere-ocean system, as computed by our model, atmospheric pO_2 could not have been higher than 0.2 PAL (Canfield and Teske 1996). This study proposed that a high rate of thermal sulfate reduction caused the rise to be anomalously low. The isotope mass balance model of the carbon and sulfur cycles was developed to determine the rate of thermal sulfate reduction required to keep atmospheric pO_2 from rising above 0.2 PAL during 2.3–2.0 Ga.

The fluctuation in the predicted atmospheric pO_2 during 2.3–2.0 Ga (Fig. 3) indicates the accumulation and subsequent drawdown of oxygen from the atmosphere-ocean system. Once the exogenic part of the sulfur cycle was established (i.e., $1/2F_{ex,S}(t) = 0$), oxygen, remaining after the oxygen consumption during the endogenic recycling of sulfate (i.e., $1/2F_{en,S}(t)$), began to accumulate in the atmosphere-ocean systems. The production of excess oxygen (i.e., $\left[F_{b,C}(t) - F_{w,C}(t)\right] + (15/8)\left[F_{b,S}(t) - F_{w,S}(t)\right]$), however, was declining, as evidenced by the decreasing slope of the rising limb. In case of the carbon cycle, $F_{w,C}(t)$ was increasing as the organic carbon reservoir grew whereas $F_{b,C}(t)$ remained the same, which results in net decrease of the term $\left[F_{b,C}(t) - F_{w,C}(t)\right]$. In case of the sulfur cycle, $F_{b,S}(t)$ was decreasing whereas $F_{w,S}(t)$

was increasing as more oceanic sulfate was reduced to sedimentary sulfides, which results in net decrease of the term $\left[F_{\mathrm{b,S}}(t)-F_{\mathrm{w,S}}(t)\right]$. Once $\left[F_{\mathrm{b,C}}(t)-F_{\mathrm{w,C}}(t)\right]+(15/8)\left[F_{\mathrm{b,S}}(t)-F_{\mathrm{w,S}}(t)\right]$ fell below $1/2F_{\mathrm{en,S}}(t)$, the inventory of atmospheric oxygen, having accumulated by that time, began to become depleted. To prevent its depletion *T* should be permitted to gradually increase so that $1/2F_{\mathrm{en,S}}(t)$ declines at the same rate as $\left[F_{\mathrm{b,C}}(t)-F_{\mathrm{w,C}}(t)\right]+(15/8)\left[F_{\mathrm{b,S}}(t)-F_{\mathrm{w,S}}(t)\right]$ and atmospheric pO_2 remains constant at a certain level.

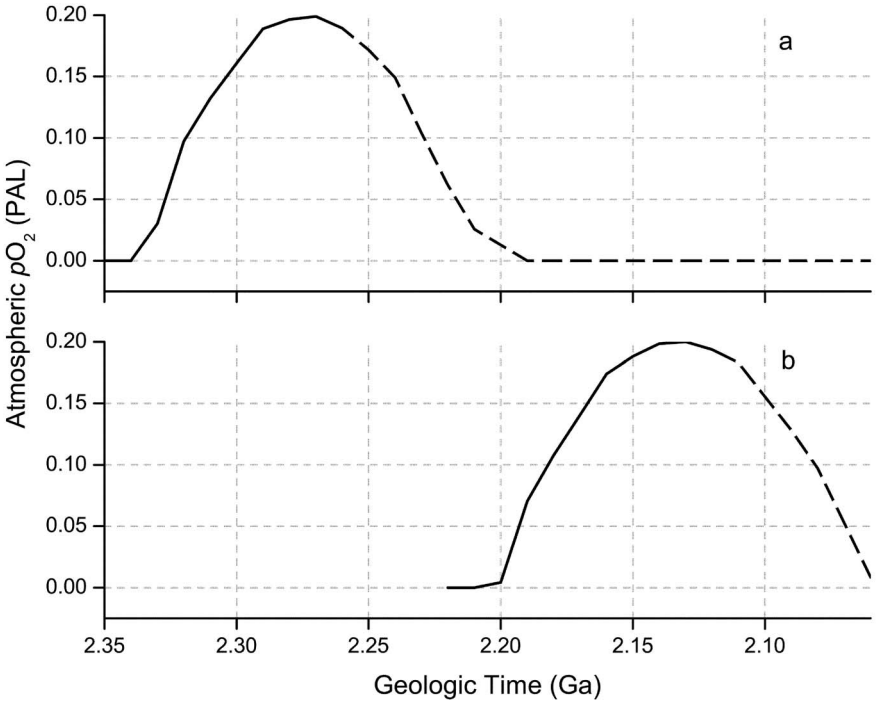

Fig. 4 Predicted rise in atmospheric pO_2 with the Lomagundi-Jatuli $\delta^{13}C$ positive excursion beginning at (a) 2.35 Ga and (b) 2.22 Ga and terminating at 2.058 Ga. The dashed portion of both curves represents the scenario when the rate of thermal sulfate reduction remains constant, i.e., does not decrease to match the decline in the production of excess oxygen

For each model run T and p were assigned different values from their uncertainty ranges and held constant during the program execution. The model was run multiple times for each combination of T and p to determine a value of n that would keep the maximum (fluctuation peak) of atmospheric pO_2 *at* 0.2 PAL during 2.3–2.0 Ga (Fig. 3). Since changing n by a tenth of a percent point causes a large change in the amplitude of the fluctuation in atmospheric pO_2, n is given in Table 1 as a one-percent-point interval containing the sought n value.

Table 1 Combinations of values of model parameters T, p, and n required to keep the maximum of atmospheric pO_2 *at* 0.2 PAL during 2.3–2.0 Ga and computed rate of thermal sulfate reduction

Run No.	T **(Ma)**	p **(%)**	n **(%)**	npS_t / T **(mol/yr)**
1	10	16	64–65	4.14×10^{12}
2	15.5	16	94–95	3.86×10^{12}
3	10	8.5	—	—

T time period required for the entire ocean to pass through the axial hydrothermal cell, p fraction that the total mass of exogenic sulfur constituted at the beginning of the Lomagundi-Jatuli $\delta^{13}C$ positive excursion from the present value S_t (4.42×10^{20} mol), n fraction of exogenic sulfur recycled endogenically

Using the model results (Table 1), the mean rate of thermal sulfate reduction was computed as npS_t / T to be roughly 4×10^{12} mol/yr, which is a *minimum* rate because atmospheric pO_2 was permitted to attain the upper limit of 0.2 PAL. The amplitude of the fluctuation in pO_2 is inversely correlated with n and highly sensitive to the change in n, i.e., a few-percent-point

decrease or increase in n causes atmospheric pO_2 to rise to biologically impermissible levels (i.e., $pO_2 > 1$ PAL) or level off (i.e., $pO_2 = 0$), respectively. Increasing n by a few percent points does not increase the rate of thermal sulfate reduction significantly. Thus, it can be concluded that the *actual* rate of thermal sulfate reduction must have been roughly 4×10^{12} mol/yr. Based on the model results, at least 65% of oceanic sulfate must have been thermally reduced, which is reasonable as shown in Shanks et al.'s (1981) 77-2 experiment of fayalite-seawater interaction (at 350°C, 500 bars, and a water/rock ratio of 40) where thermal reduction of aqueous sulfate (29 mmol/kg) was nearly complete.

The rise in atmospheric pO_2 could have been not only dramatic in its magnitude but also rapid. Had the Lomagundi-Jatuli $\delta^{13}C$ positive excursion begun at 2.35 Ga, atmospheric pO_2 would have reached the upper limit before 2.25 Ga (Fig. 3a), which contradicts the paleosol record suggesting that the atmosphere became oxygenated after 2.25 Ga (Holland 1999). Therefore, it can be concluded that the Lomagundi-Jatuli event began somewhere closer to 2.22 Ga (Fig. 3b).

The model results (Table 1) also show that the abundance of oceanic sulfate must have been close to the saturation point contrary to the notion of a sulfate-poor Paleoproterozoic ocean based on the sulfur isotope fractionations' being smaller in the Precambrian than in the Phanerozoic, which purportedly indicates that the concentration of oceanic sulfate was lower during that time (Strauss 2004) since the isotopic fractionation depends on the substrate abundance (Petsch 2004), and the absence of massive sulfate evaporites of the Paleoproterozoic age (Strauss 2004). The former argument would be valid only if the sulfate reducing bacterium were the only microorganism fractionating sulfur isotopes. The isotopic fractionation between Phanerozoic sulfates and sulfides, however, is often a cumulative of fractionations imparted by

sulfate-reducing and elemental sulfur-disproportionating bacteria (Canfield and Thamdrup 1994), which can account for up to 70% of the sulfur isotopic fractionation (Johnston et al. 2005). Thus, the inviability of elemental sulfur-disproportionating bacteria in the Precambrian can explain the smaller sulfur isotope fractionations. As for the absence of massive sulfate evaporites of the Paleoproterozoic age, it can also be explained by the lack of geographical features (e.g., lagoons) required for the deposition of evaporites, which is the situation occurring at present (Brimblecombe 2004). Therefore, although there is no direct evidence to support a view that the ocean contained a high abundance of sulfate during 2.3–2.0 Ga, there is no direct evidence to refute it either.

REFERENCES

Bekker A, Holland HD, Wang PL, Rumble III D, Stein HJ, Hannah JL, Coetzee LL, Beukes NJ (2004) Dating the rise of atmospheric oxygen. Nature 427:117–120

Berner RA (2004) The Phanerozoic carbon cycle: CO_2 and O_2. Oxford University Press, New York

Brimblecombe P (2004) The global sulfur cycle. In: Schlesinger WH (ed) Treatise in geochemistry: Biogeochemistry, Elsevier Pergamon, San Diego, pp 645–682

Canfield DE, Teske A (1996) Late Proterozoic rise in atmospheric oxygen concentration inferred from phylogenetic and sulphur-isotope studies. Nature 382:127–132

Canfield DE, Thamdrup B (1994) The production of 34S-depleted sulfide during bacterial disproportionation of elemental sulfur. Science 266:1973–1975

Farquhar J, Bao H, Thiemens M (2000) Atmospheric influence of Earth's earliest sulfur cycle. Science 289:756–758

Fennel K, Follows M, Falkowski PG (2005) The co-evolution of the nitrogen, carbon and oxygen cycles in the Proterozoic ocean. American Journal of Science 305:526–545

Freeze RA, Cherry JA (1979) Groundwater. Prentice-Hall, Englewood Cliffs

Garrels RM, Lerman A (1984) Coupling of the sedimentary sulfur and carbon cycles—an improved model. American Journal of Science 284:989–1007

Hayes JM, Lambert IB, Strauss H (1992) The sulfur-isotopic record. In: Schopf JW, Klein C (eds) The Proterozoic biosphere: A multidisciplinary study, Cambridge University Press, Cambridge, pp 129–132

Holland HD (1999) When did the Earth's atmosphere become oxic? A reply. Geochemical News 100:20–22

Holland HD (2006) The oxygenation of the atmosphere and oceans. Philosophical Transactions of the Royal Society B 361:903–915

Johnston DT, Farquhar J, Wing BA, Kaufman AJ, Canfield DE, Habicht KS (2005) Multiple sulfur isotope fractionations in biological systems: A case study with sulfate reducers and sulfur disproportionators. American Journal of Science 305:645–660

Karhu JA, Holland HD (1996) Carbon isotopes and the rise of atmospheric O_2. Geology 24:867–870

Kasting JF (1987) Theoretical constraints on oxygen and carbon dioxide concentrations in the Precambrian atmosphere. Precambrian Research 34:205–229

Lowell RP, Keller SM (2003) High-temperature seafloor hydrothermal circulation over geologic time and Archean banded iron formations. Geophysical Research Letters 30:44.1–44.4

Melezhik VA, Fallick AE, Hanski EJ, Kump LR, Lepland A, Prave AR, Strauss H (2005) Emergence of the aerobic biosphere during the Archean-Proterozoic transition: Challenges of future research. GSA Today 15:4–11

Melezhik VA, Huhma H, Condon DJ, Fallick AE, Whitehouse MJ (2007) Temporal constraints on the Paleoproterozoic Lomagundi-Jatuli carbon isotopic event. Geology 35:655–658

Petsch ST (2004) The global oxygen cycle. In: Schlesinger WH (ed) Treatise in geochemistry: Biogeochemistry, Elsevier Pergamon, San Diego, pp 645–682

Shanks III WC, Bischoff JL, Rosenbauer RJ (1981) Seawater sulfate reduction and sulfur isotope fractionation in basaltic systems: Interaction of seawater with fayalite and magnetite at 200–350°C. Geochimica et Cosmochimica Acta 45:1977–1995

Shields G, Veizer J (2002) Precambrian marine carbonate isotope database: Version 1.1. Geochemistry, Geophysics, Geosystems 3:1–12

Stein CA, Stein S, Pelayo A (1995) Heat flow and hydrothermal circulation. In: Humphris SE, Zierenberg RA, Mullineaux LS, Thomson PE (eds) Seawater hydrothermal systems: Physical, chemical, biological, and geological interactions, American Geophysical Union, Washington, DC, pp 425–445

Strauss H (1993) The sulfur isotopic record of Precambrian sulfates: New data and a critical evaluation of the existing record. Precambrian Research 63:225–246

Strauss H (2004) 4 Ga of seawater evolution: Evidence from the sulfur isotopic composition of sulfate. In: Amend JP, Edwards KJ, Lyons TW (eds) Sulfur biogeochemistry: Past and present, Geological Society of America, Boulder, CO, pp 195–205

Veizer J (1988) The evolving exogenic cycle. In: Gregor CB, Garrels RM, Mackenzie FT, Maynard JB (eds) Chemical cycles in the evolution of the Earth, John Wiley and Sons, New York, pp 75–219

APPENDIX A: COMPUTATION OF ATMOSPHERIC PO_2

Based on the Henry's Law, the concentration of O_2 dissolved in the surface ocean is directly proportional to atmospheric pO_2:

$$\frac{m_s}{A_o d} = \frac{m_a g k}{A_e}, \tag{30}$$

where m_s is the quantity of O_2 dissolved in the surface ocean (mol), m_a is the quantity of O_2 in the atmosphere (mol), g is acceleration due to gravity (9.81 m/s^2), A_e is the surface area of the Earth (5.1×10^{14} m^2), A_o is the area of the surface ocean $(0.7A_e)$, d is the depth of the surface ocean (70 m), and k is the Henry's Law constant taken from Sander (1999) to be 1.3×10^{-8}

mol/m^3/Pa at 25 °C. The quantity of O_2 in the atmosphere-ocean system (m), computed via the model, is:

$$m = m_s + m_a \,. \tag{31}$$

Solving the system of Eqn. (30) and (31) for m_a yields:

$$m_a = m \frac{A_e}{A_e + gkA_o d} \,. \tag{32}$$

Instead of recording m and m_a, the model records m / m_0 and m_a / m_{a0}, where m_0 and m_{a0} are the present quantity of O_2 in the atmosphere-ocean system and atmosphere, respectively. The fraction in Eqn. (32) is constant and hence the two ratios are equal. The present atmospheric level (1 PAL), i.e., m_{a0}, is 3.8×10^{19} mol.

APPENDIX B: MODEL SOURCE CODE

```
//Header file (.h)
class AtmOcean;
class C;
class S;

/*************************************************************
```

```
PUBLIC CONSTANTS:
START_T, start time of the modeling period (Ga)
END_T, end time of the modeling period (Ga)
STEP, model time step (Ga)
*************************************************************/
const double START_T = 2.22;
const double END_T = 2.058;
const double STEP = 0.031/2;
const double O2toSulfide = 15.0/8.0;
const double O2toSO2 = 1.0/2.0;

class S{
private:
     static const double p;
     static const double St;
     static const double n;
     static const double alpha;
     static const double k;
     double So;
     double Sp;
     double Dp;
     double t;
     double Fb(AtmOcean* AtmOceanObj);
     double Fw(void);
```

```
     double Fex(AtmOcean* AtmOceanObj);
     double Fen(AtmOcean* AtmOceanObj);
     double Do(double T) const;
     void cycle(AtmOcean* AtmOceanObj);
public:
     S(void);
     friend void interact(AtmOcean* AtmOceanObj, S* SObj, C*
ExoCObj);

};

class C{
private:
     static const double Ct;
     static const double k;
     static const double f;
     double t;
     double Co;
     double Fb(void);
     double Fw(void);
     void cycle(AtmOcean* AtmOceanObj);
public:
     C(void);
```

```
     friend void interact(AtmOcean* AtmOceanObj, S* SObj, C*
ExoCObj);
};

class AtmOcean{
private:
     double t;
     double O2;
public:
     friend class C;
     friend class S;
     AtmOcean(void);
     friend void interact(AtmOcean* AtmOceanObj, S* SObj, C*
ExoCObj);
};
//Source file (.cpp)
#include "reserv.h"
#include <math.h>
#include <algorithm>
#include <fstream>
#include<iostream>
#include <iomanip>

double pO2 (double O2);
```

```
const double C::Ct = 6.5e21;
const double C::k = 1.6; //Ga^-1
const double C::f = 0.37;
const double S::p = 0.16;     //fraction the mass of aqueous S
                              constitutes //from the total mass of
                              exogenic S
const double S::St = 4.42e20;
const double S::alpha = 20;
const double S::k = 1.6;
const double S::n = 0.94;     //fraction of S recycled
endogenically

//EXOGENIC C CYCLE
C::C(void){
     t = START_T;
     Co = 0.14 * Ct;
}

double C::Fb(void){
     return STEP * k * f * Ct;
}

double C::Fw(void){
     return STEP * k * Co;
```

```
}

void C::cycle(AtmOcean* AtmOceanObj){
     AtmOceanObj->O2 += (Fb() - Fw());
     Co = Co + (Fb() - Fw());
}

//S CYCLE
S::S(void){
     t = START_T;
     So = 0;
     Sp = 0;
     Dp = 0;
}

double S::Do(double T) const{
     const double slope = (25.0 - 2.0)/(1.6 - START_T);
     const double y_intercept = 2.0;
     return slope * (T - START_T) + y_intercept;
}

double S::Fex(AtmOcean* AtmOceanObj){return std::min((1-
n)*(p*St)-So-Sp, AtmOceanObj->O2/O2toSO2);}
```

```
double S::Fen(AtmOcean* AtmOceanObj){return std::min(n*(p*St),
AtmOceanObj->O2/O2toSO2);}

double S::Fb(AtmOcean* AtmOceanObj){
     const double Dt = 2;
     return ((Do(t-STEP) - Do(t)) * So + (Do(t-STEP) - Dp) *
Fw() + (Do(t-STEP) - Dt) * Fex(AtmOceanObj))/alpha;
}

double S::Fw(void){
     return k * STEP * Sp;
}

void S::cycle(AtmOcean* AtmOceanObj){
     const double Dt = 2;
     double dSo_dt = Fw() - Fb(AtmOceanObj) + Fex(AtmOceanObj);
     double dSp_dt = Fb(AtmOceanObj) - Fw();
     double dDp_dt = ((Do(t-STEP) - alpha) * Fb(AtmOceanObj) -
Dp * Fb(AtmOceanObj))/(Sp + dSp_dt);

     AtmOceanObj->O2 -= O2toSulfide * dSo_dt;
     AtmOceanObj->O2 -= O2toSO2 * Fen(AtmOceanObj);

     So = So + dSo_dt;
```

```
	Sp = Sp + dSp_dt;
	Dp = Dp + dDp_dt;
}

//ATM-OCEAN SYSTEM
AtmOcean::AtmOcean(void){
	t = START_T;
	O2 = 0;
}

void interact(AtmOcean* AtmOceanObj, S* SObj, C* CObj){
	const double OUT_UNIT = 1e8;  //output every 100 Ma
	const double m_oc = 1.37e21;  //ocean mass (kg)
	const double solub = 0.051;   //0.051 mol S/kg H2O
	int i = 0;
	double t;
	std::ofstream out;
	out.open("OUT.TXT");
	out<<std::setprecision(3);
	for(t = START_T; t >= END_T; t -= STEP)
	{
		AtmOceanObj->t = t;
		SObj->t = t;
		CObj->t = t;
```

```
            out<<t<<'\t';
            out<<pO2(AtmOceanObj->O2)<<'\t';
            CObj->cycle(AtmOceanObj);
            SObj->cycle(AtmOceanObj);
            out<<'\n';
      }
      out.close();
}

double pO2 (double O2){ //in PAL
      const double g = 9.81;   //acceleration due to gravity
(m/s^2)
      const double k = 4.2e-7;//Henry's law constant (kg/m^3/Pa)
at 15 deg C
      const double Ae = 5.1e14;//Surface area of the Earth (m^2)
      const double Ao = 3.6e14;//Surface area of the ocean (m^2)
      const double d = 70;     //Depth of the surface ocean (m)
      const double c1 = 0.032;//conversion factor for O2 (kg/mol)
      const double c2 = 1.01e5;//conversion factor (Pa/bar)
      const double PAL = 0.21;//present atmopsheric level (bar)
      return (O2 * c1 * g)/(Ae + g * k * Ao * d)/c2/PAL;

}
```